

A fast and accurate generalized analytical approach for PV arrays modeling under partial shading conditions

Mostefa Kermadi ^{a,*}, Vun Jack Chin ^b, Saad Mekhilef ^{a,c,*}, Zainal Salam ^d

^a Power Electronics and Renewable Energy Research Laboratory (PEARL), University of Malaya, 50603 Kuala Lumpur, Malaysia

^b School of Electronics and Computer Science, University of Southampton Malaysia, 79200 Iskandar Puteri, Malaysia

^c School of Software and Electrical Engineering, Swinburne University of Technology, Victoria, Australia

^d Centre of Electrical Energy Systems, School of Electrical Engineering, Universiti Teknologi Malaysia, 81310 Johor Bahru, Malaysia



ARTICLE INFO

Keywords:

Photovoltaics
Partial shading condition
Parameter extraction
Bypass and blocking diode
PV array modeling

ABSTRACT

This paper proposes a generalized analytical approach to model the photovoltaic (PV) arrays under partial shading conditions (PSC). The proposed method is simple: it requires only the standard test condition (STC) parameters of the PV modules and the irradiance level imposed on each module. By using this information, the *P-V* and *I-V* curves of shaded PV arrays are obtained by simple steps. Firstly, the current-voltage (*I-V*) curves for all assembled submodules receiving the same level of irradiance are generated using the two-diode model. The parameters of the latter are computed using a fast parameter extraction method. Secondly, the *I-V* curve of each shaded string is computed using the computed *I-V* curves of its submodules. In the last step, the resulted *I-V* curve of the array is obtained by summation of all *I-V* strings curves. The proposed method is simple, fast, and can be coded in any development platform. Besides, the prediction accuracy is enhanced by incorporating the real effect of bypass and blocking diodes in the model. Furthermore, the proposed method could be generalized for any number of series/parallel connections in a shaded PV array. The method can be useful to generate critical shading patterns for maximum power point tracking (MPPT) algorithms evaluation. It can also be used as a tool to obtain instant shading patterns in PV array simulators.

1. Introduction

Photovoltaic (PV) systems are being increasingly employed in many applications such as distributed power generation, building-integrated PV (BIPV), and standalone systems for remote/rural areas (Shukla et al., 2017; Chin and Salam, 2019). However, PV installations are prone to shadings due to the passing cloud, dust/soiling, or by obstructing objects such as trees and buildings. This condition results in a phenomenon known as partial shading. When an array is partially shaded, the power-voltage (*P-V*) characteristics curve exhibits multiple power peaks, i.e., several local peaks (LP) and a global maximum power point (GMPP). As a result, the maximum power point tracking (MPPT) task becomes more complicated because it has to discriminate between the two and ensures that the operation at a local peak is avoided. Consequently, if the MPPT is not correctly implemented, the energy yield will be significantly affected. Due to the importance of this issue, it is not surprising that the partial shading is still among the sought-after topic in

PV systems. There is a need to study, understand, and investigate the effect of partial shading in order to improve the performance of the MPPT algorithm. Furthermore, a holistic understanding of the partial shading allows for its effective mitigation.

Typically, the PV module/array models are developed to predict the behavior of PV arrays under uniform and non-uniform insolation conditions (partial shading). There are two approaches to compute the electrical characteristics of the PV array: component-based and analytical-based approaches. For the component-based approach, a general-purpose simulation software such as Simulink is commonly used. The PV array model is typically built by interconnecting the ready-to-use components (current sources, diodes, and resistors) from the drop-down menu of the component library. For example, authors in Ishaque et al. (2011a) designed a PV simulator based on the Simulink model that incorporates the component models from the SimPowerSystems blocks. The models can be characterized using a pop-up form that requires the user to enter the relevant parametric PV cell values. Generally, the software is equipped with extensive post-

* Corresponding authors at: Power Electronics and Renewable Energy Research Laboratory (PEARL), University of Malaya, 50603 Kuala Lumpur, Malaysia (M. Kermadi and S. Mekhilef).

E-mail address: mostefa@um.edu.my (M. Kermadi).

Nomenclature	
I_{PV}	photocurrent
R_p	shunt resistance
R_s	series resistance
I_o	saturation current of the diode
α	ideality factor of the diode
V_T	thermal potential
k	Boltzmann constant
T	the temperature in kelvin (K)
q	the electron charge
N_s	number of series-connected PV cells per module
K_i	temperature coefficient of the short-circuit current
K_v	temperature coefficient of the open circuit voltage
$P_{max,c}$	calculated maximum power from model
$P_{max,e}$	experimental maximum power from datasheet
tol	error tolerance
SDP	section dividing point
$str(i)$	i^{th} string
V_D	voltage across diode
V_{fwd}	forward voltage of diode
R_{on}	equivalent on-resistance of diode in conduction mode
I_D	current passes through a diode
$I_{sc-array}$	short circuit current of a PV array
$V_{oc-array}$	open-circuit voltage of a PV array
I_{array}	current of a PV array
P_{array}	power of a PV array
$V_{oc-str(j)}$	open-circuit voltage of a string j
$I_{sc-str(j)}$	short circuit current of a string j
$V_{str(j)}$	voltage of a string j
$I_{str(j)}$	current of a string j

processing tools for extended analysis and graphical representation. Despite the user-friendliness and flexibility, the program execution is quite slow. The array simulation may require several seconds range for short PV strings and tens of seconds for longer strings. Furthermore, for every test, the user needs to key in the irradiance value for all modules, waits for the completion of a simulation run, before getting the output characteristics of the entire array. These processes are especially troublesome when the array is subjected to partial shading conditions.

On the other hand, the analytical-based approach involves the formulation of a mathematical relationship for the equivalent circuit model of PV cells and diodes. In effect, it replaces the electrical components of the models by equations and relates them to the environmental parameters such as irradiance and temperature. These equations are coded and integrated into the simulator using Matlab or other programming languages. It has a much faster execution time, but it is not as flexible as the component-based approach. Thus, the analytical method is customarily used to model specific and intricate components of the system; for example, the PV array itself. The remaining part of the system is still built using the component model from the drop-down menu of the software.

To date, several attempts are made to predict the PV system output using the analytical approach. Works in Wang and Hsu (2010), Dadje et al. (2018), Seyedmahmoudian et al. (2013) attempted to provide analytical models for PV arrays under partial shading based on the equivalent electrical circuit models of PV cells. However, these studies are carried out on a single string composed of two or three series-connected modules. There is no generalized formula derived. In addition to that, the effects of bypass and blocking diodes are not considered. In Diqing et al. (2012), an analytical model to estimate the global output power of the shaded PV module versus the number of bypass diodes is proposed. Despite the inclusion of the latter, the real effect of bypass and blocking diodes are not studied rigorously. Furthermore, the proposed modeling approach is not generalizable for any series-parallel array configuration. In Quaschning and Hanitsch (1996), an accurate numerical algorithm to simulate the complex characteristics of shaded modules was proposed. However, the accuracy comes at the expense of considerable computation effort. In another work, authors in Patel and Agarwal (2008) proposed a Matlab-based code for PV arrays modeling under partial shading. However, the procedures to obtain the P-V curves are not adequately described. Recently, an MPPT scheme that utilized the analytical model of PV system under partial shading is proposed (Xenophontos and Bazzi, 2018; Arjun et al., 2019). Despite the successful tracking of the global maximum power point (GMPP), the effect of bypass and blocking diodes are not incorporated into the model. Furthermore, the method requires information on the irradiance on each group of cells, which implies the need for multiple irradiance sensors,

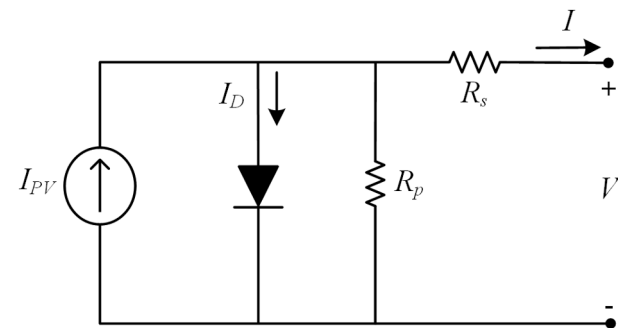


Fig. 1. The single diode R_p -model of PV module.

and consequently, limits the practical implementation of such methods.

From the above discussion, it is clear that the scope of the analytical approach for PV array modeling is quite limited. None of the previous works attempt to provide a generalized modeling approach that is applicable for any number of series-parallel array receiving various irradiance values. Also, none of them tried to incorporate the effect of bypass and blocking diodes in their models. In view of these shortcomings, this work proposes a fast, accurate, and generalized analytical approach to model the PV array under partial shading. The work has several merits: first, it can be generalized for any series-parallel array configuration under any partial shading condition. Second, it enhances the accuracy of the I - V and P - V characteristics of shaded arrays by incorporating the effect of the blocking and bypass diodes. The execution of the analytical equations is very fast and it can be coded in any development platform. Thus, it can suitably be integrated as one of the components in a PV computer-aided design tool. Alternatively, the algorithm can also be adopted in commercial PV simulators as a graphical-user-interface to generate instantaneous shading patterns from a profile that contains different irradiance levels.

The remaining of the paper is organized as follows: In Section 2, the two-diode equivalent model used along with a fast parameter extraction method are described. The proposed generalized analytical approach for PV arrays modeling under partial shading conditions is presented in Section 3. The advantages of the proposed approach over conventional component-based simulation method are exposed in Section 4. Finally, a Conclusion is made in the last Section.

2. Equivalent model of the PV module

In this Section, a simple and efficient parameter estimation method

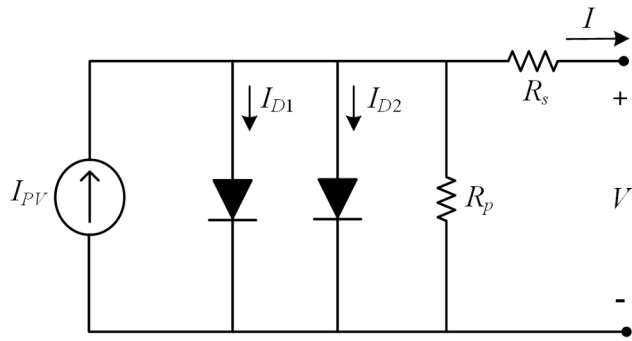


Fig. 2. The two-diode model of PV module.

for PV cells under uniform insolation using the two-diode model is derived. Before moving further, it is beneficial to revisit a simpler model, i.e., the single-diode, as shown in Fig. 1. The current source represents the light-generated electric current, known as the photocurrent (I_{PV}). The ideal diode describes the electrical characteristics of the p - n junction in the PV cell. On the other hand, the series resistance (R_s) accounts for the cumulative resistance along the current flow path (e.g., a contact resistance between the silicon and electrodes surfaces, the resistivity of the silicon material and electrodes). The shunt resistance (R_p) corresponds to the leakage current in the p - n junction. By Kirchhoff's current law, the output current of the one-diode model is described by Eq. (1).

$$I = I_{PV} - I_o \left[e^{\frac{V+IR_s}{aV_T}} - 1 \right] - \frac{V + IR_s}{R_p} \quad (1)$$

where I_o is the saturation current and a is the diode ideality factor. $V_T = N_s kT/q$ represents the thermal potential, where k is the Boltzmann constant ($1.3806503 \times 10^{-23}$ J/K), T is the temperature in kelvin (K), and q is the electron charge ($1.60217646 \times 10^{-19}$ C). N_s denotes the number of series-connected PV cells per module. In total, the model contains five parameters, i.e., I_{PV} , I_o , a , R_s , and R_p , which define the I - V characteristics of the PV cell.

Owing to its simplicity (i.e., only requires the determination of five unknown parameters), the one-diode model is among the most widely used PV cell model (Villalva et al., 2009; Chin et al., 2015a). However, for a more realistic description of the PV cell characteristics, the two-diode PV model is a preferred choice (Ishaque et al., 2011b; Chin et al., 2017a; Prasanth Ram et al., 2020). The inclusion of an extra diode considers the recombination process in the space-charge region that is neglected in the single-diode model (Chin et al., 2015c). The equivalent circuit for the two-diode model is shown in Fig. 2. The output current of the cell is given by

$$I = I_{PV} - I_{o1} \left[e^{\frac{V+IR_s}{a_1 V_T}} - 1 \right] - I_{o2} \left[e^{\frac{V+IR_s}{a_2 V_T}} - 1 \right] - \frac{V + IR_s}{R_p} \quad (2)$$

where I_{o1} , a_1 , and I_{o2} , a_2 denote the saturation current, ideality factor of the first and second diode, respectively. In total, seven unknown parameters in the model are required to be determined, i.e., I_{PV} , I_{o1} , I_{o2} , a_1 , a_2 , R_s , and R_p . The two-diode model has gained significant attention in recent years due to its improved accuracy, particularly at low irradiance levels (Chin et al., 2015b, 2016).

2.1. Parameter extraction

The first step in the analytical approach is to calculate the output characteristics of the PV modules under uniform irradiance. For this, the parameters of the equivalent circuit must be known. Thus, an efficient and accurate parameter extraction method is required. For the two-diode model, the extraction method proposed by Ishaque et al. (2011b) is widely utilized. To make the two-diode model analytically manageable, the following assumptions are made: $I_{o1} = I_{o2} = I_o$ and $(a_1$

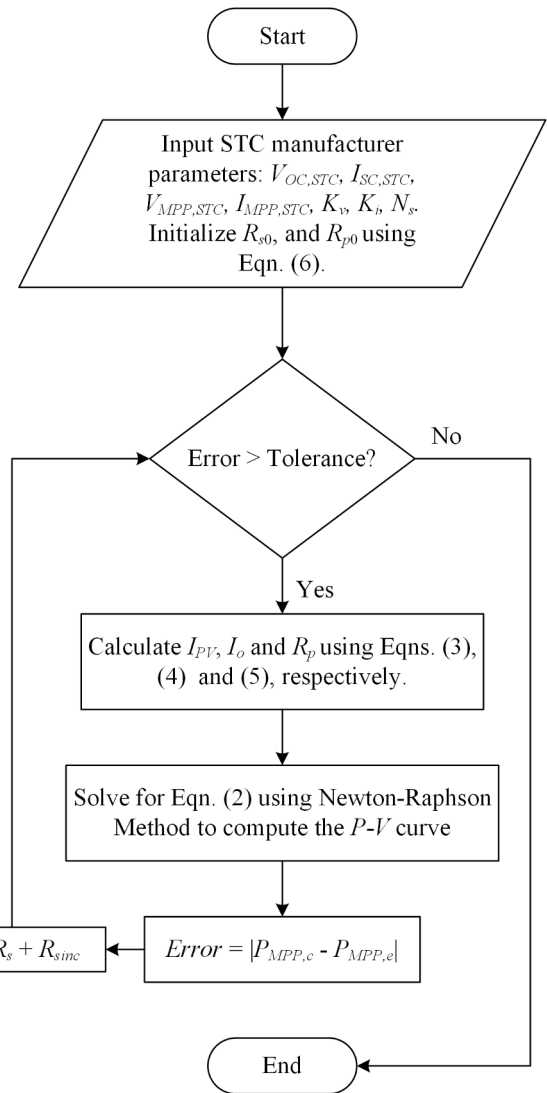


Fig. 3. Parameter extraction algorithm for the two-diode model.

$+ a_2)/p = 1$. Furthermore, the value of a_1 is assumed to be unity (following the Shockley diode diffusion theory (Chih-Tang et al., 1957)), while a_2 is assigned an arbitrary value greater than 1.2. Based on these assumptions, the two-diode model equation can be simplified as in Eq. (3).

$$I = I_{PV} - I_o \left(e^{\frac{V+IR_s}{V_i}} + e^{\frac{V+IR_s}{(p-1)V_i}} + 2 \right) - \frac{V + IR_s}{R_p} \quad (3)$$

The values for I_{PV} and I_o are determined based on the expressions described in Villalva et al. (2009):

$$I_{PV} = \frac{G}{G_{STC}} [I_{SC,STC} + K_i(T - T_{STC})] \quad (4)$$

$$I_o = \frac{I_{SC,STC} + K_i(T - T_{STC})}{\exp \left[\frac{V_{OC,STC} + K_v(T - T_{STC})}{(a_1 + a_2)V_i/p} \right] - 1} \quad (5)$$

where G denotes irradiance (W/m^2). The STC subscripts represent values measured at Standard Test Conditions—which are characterized by solar irradiance of 1 kW and module temperature of 298.15 K. Meanwhile, K_i and K_v are the temperature coefficients of the short-circuit current and open-circuit voltage, respectively.

The remaining two unknown parameters, i.e., R_s and R_p , are

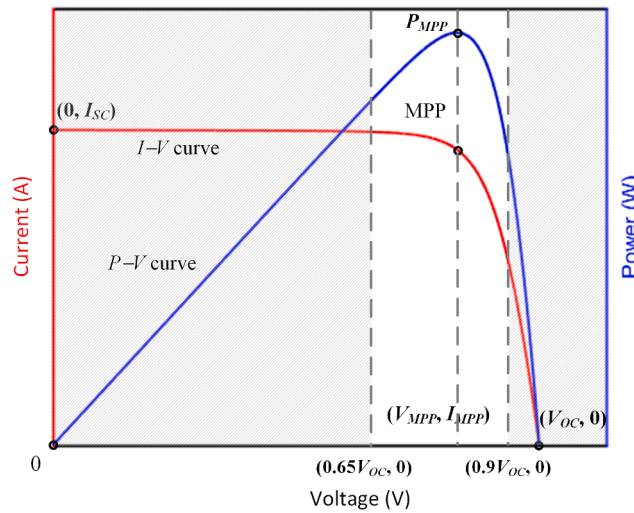


Fig. 4. Reduced MPP search range according to ASR.

computed utilizing a simple iterative algorithm illustrated in Fig. 3. The value of R_s is incremented by R_{sinc} starting from zero, and the corresponding values of I_{PV} , I_o , and R_p are computed based on Eqs. (4)–(6), respectively. Subsequently, the P - V curve is computed using the Newton-Raphson Method (NRM) to evaluate the difference between the calculated ($P_{max,c}$) and maximum experimental power ($P_{max,e}$). The calculated maximum power is the maximum element in the product of the voltage and current vectors—for example, this can easily be determined using the “`max()`” function in MATLAB. On the other hand, the maximum experimental power is the rated maximum power specified on the manufacturer datasheet. The algorithm is reiterated until the difference falls within a predefined error tolerance, tol . Since the maximum power values specified on the datasheet are typically given in two decimal places, a tol of 0.001 would suffice. Further, we found this value to provide the right balance between accuracy and computational speed. Eq. (6) determines the value of R_p , (6), which is obtained by rearranging the terms of the model equation at maximum point power. Meanwhile, the initial values of the series (R_{s0}) and shunt resistances (R_{p0}) are set according to Eq. (7). The latter estimates the minimum value of R_p from the slope of the line segment between the short-circuit and the maximum power points (Villalva et al., 2009).

$$R_p = \frac{V_{MPP} + I_{MPP} R_s}{I_{PV} - I_o \left[e^{\frac{V_{MPP} + I_{MPP} R_s}{V_t}} + e^{\frac{V_{MPP} + I_{MPP} R_s}{(p-1)V_t}} + 2 \right] - \frac{P_{MPP,e}}{V_{MPP}}} \quad (6)$$

$$R_{s0} = 0; R_{p0} = \frac{V_{MPP,STC}}{I_{SC,STC} - I_{MPP,STC}} - \frac{V_{OC,STC} - V_{MPP,STC}}{I_{MPP,STC}} \quad (7)$$

2.2. Modifications to accelerate the parameter extraction algorithm

For improved computation speed, this paper implements the modifications that were proposed in Chin and Salam (2018), Chin et al. (2017b)—namely, the Adaptive Search Range (ASR) and the Improved Newton-Raphson Method (iNRM). The first modification reduces the computational burden of the algorithm by minimizing the area of the P - V curve to be computed on every iteration. Based on an extensive survey, the study suggests that plotting only a fraction of the curve, i.e., from 65% to 90% of open-circuit voltage, is adequate for the purpose of maximum power point matching. Fig. 4 illustrates the “crucial” region of the P - V curve, according to ASR.

On the other hand, the second modification (i.e., iNRM) introduces a simple procedure to improve the computation of the I - V curve (Chin et al., 2017b). Due to the transcendental nature of Eq. (3), a root-finding algorithm is required to solve for the corresponding value of current for

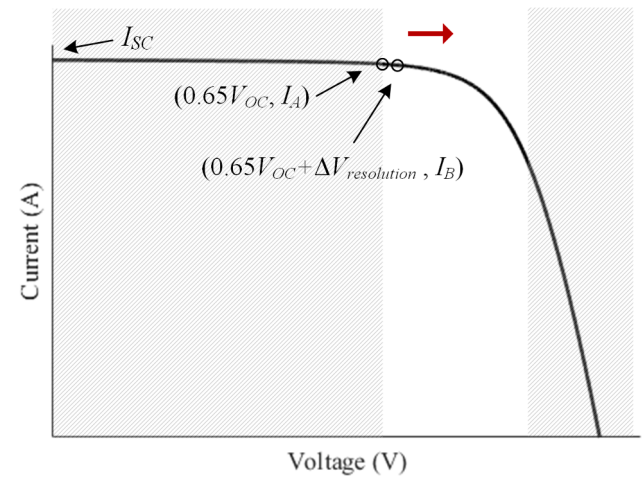


Fig. 5. Illustration of the rationale behind the iNRM initialization procedures.

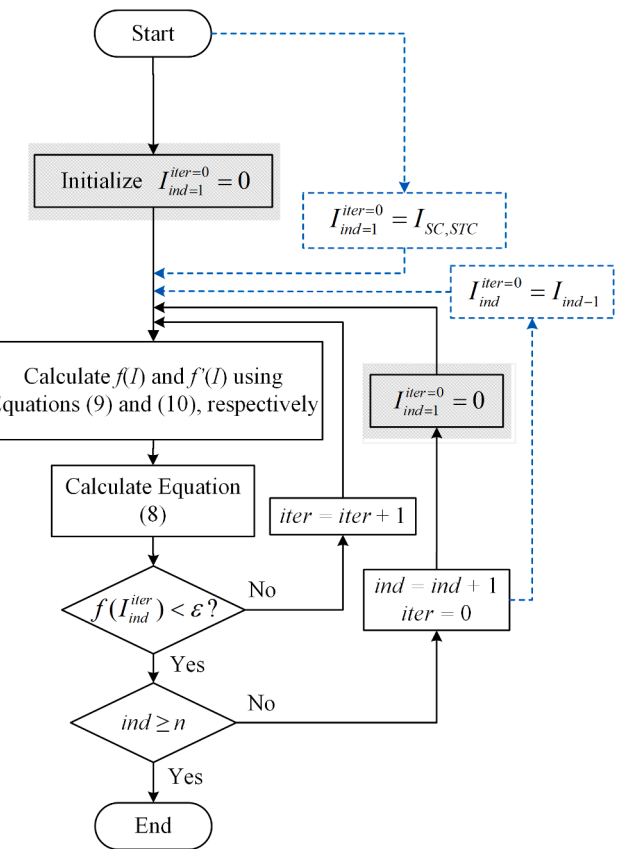


Fig. 6. The flowchart of the iNRM (Chin et al., 2017b).

each voltage point of interest. Conventionally, NRM is employed using Eqs. (8)–(10).

$$I_{ind}^{iter+1} = I_{ind}^{iter} - \frac{f(I_{ind}^{iter})}{f'(I_{ind}^{iter})} \quad (8)$$

where subscript “ ind ” indicates the element index of vector I , and superscript “ $iter$ ” describes the iteration number; and,

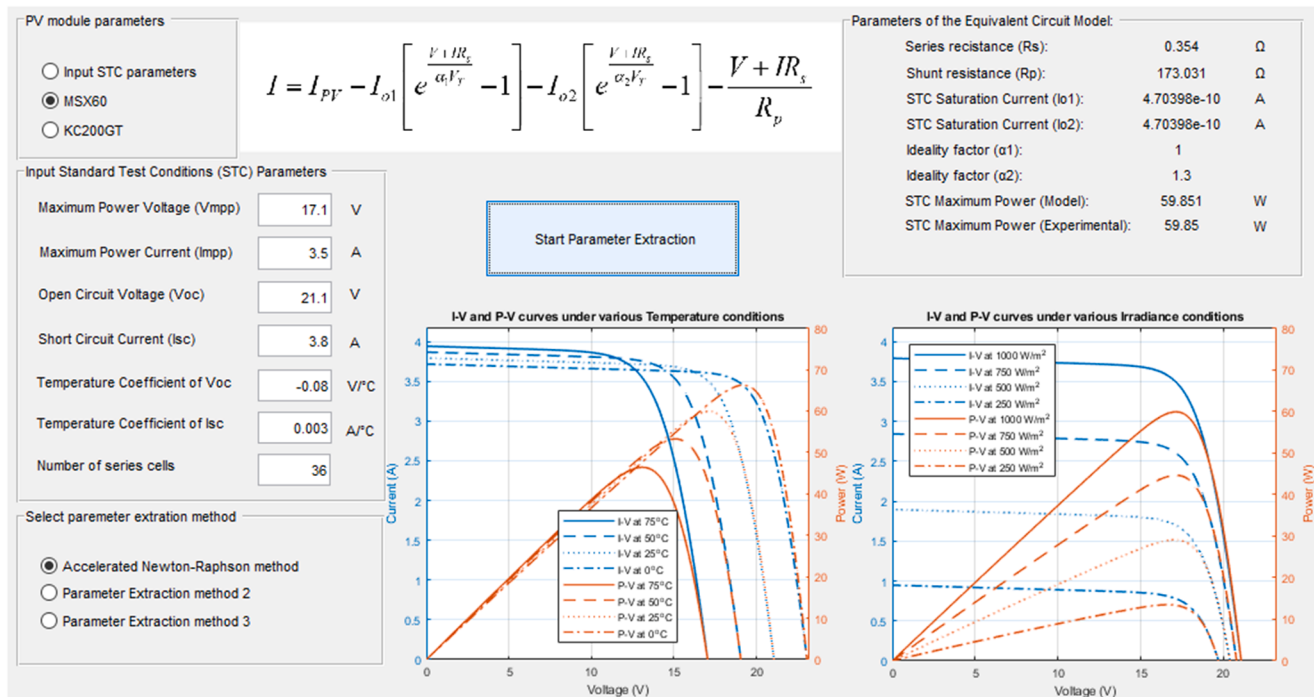


Fig. 7. Graphical-user interface of the Accelerated Newton-Raphson parameter extraction method.

$$f(I_{ind}^{iter}) = I_{PV} - I_o \left(e^{\frac{V+I_{ind}^{iter}R_s}{V_t}} + e^{\frac{V+I_{ind}^{iter}R_s}{(p-1)V_t}} + 2 \right) - \frac{V + I_{ind}^{iter}R_s}{R_p} - I_{ind}^{iter} \quad (9)$$

$$f'(I_{ind}^{iter}) = -\frac{I_o R_s}{V_t} e^{\frac{V+I_{ind}^{iter}R_s}{V_t}} - \frac{I_o R_s}{(p-1)V_t} e^{\frac{V+I_{ind}^{iter}R_s}{(p-1)V_t}} - \frac{R_s}{R_p} - 1 \quad (10)$$

In the traditional implementation of the NRM for computing the I - V curve, it is customary to set the initial value of I as zero (Eq. (11)) irrespective of the voltage value (Villalva et al., 2009; Walker, 2001; Jing Jun and Kay-Soo, 2012).

$$I_{ind}^{iter=0} = 0, \quad ind = 1, 2, 3 \dots n \quad (11)$$

However, as shown in Fig. 4, for the majority of the voltage range, the PV module operates at current much higher than zero. Therefore, although Eq. (11) does not hinder the algorithm's ability to find the root, it causes I to be initiated far from the real solution (Chin et al., 2017b). As a result, the conventional NRM routine is needlessly slow and inefficient. To eliminate this drawback, the gist of iNRM is to initiate I in the vicinity of the final solution to minimize the number Newton-Raphson iterations (Chin et al., 2017b). As illustrated in Fig. 5, the first solution for current, at $0.65V_{OC}$ (denoted as I_A), is in the vicinity of I_{SC} . Therefore, a reasonable initial guess for I_A would be $I_{ind=1}^{iter=0} = I_{SC,STC}$. On the other hand, given the continuous nature of Eq. (3), it can be deduced that the subsequent solution for I (represented as I_B in the figure) will be in the neighborhood of the preceding solution. Hence, the initial value for each successive point of I (i.e. $ind = 2, 3, 4 \dots n$), can be defined as $I_{ind}^{iter=0} = I_{ind-1}$. The flowchart of the iNRM is as shown in Fig. 6. Note that the proposed modifications blocks (enclosed in dashed lines) are executed in place of the greyed-out blocks of the NRM algorithm. Fig. 7 shows the graphical-user interface developed for parameters extraction of the two diode model.

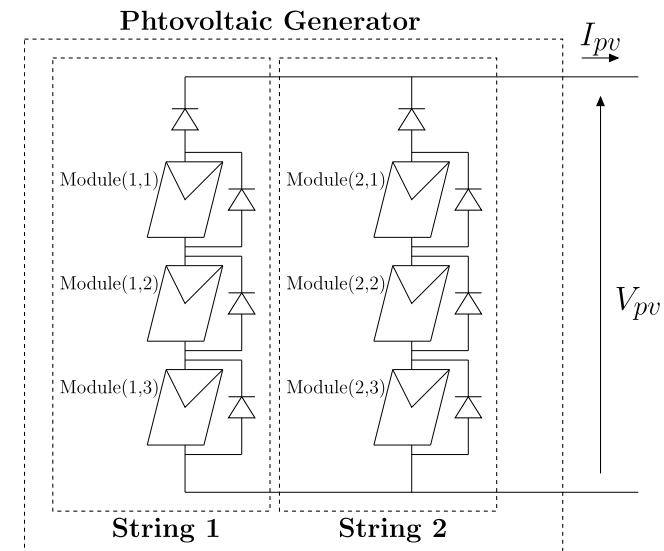


Fig. 8. Shaded PV array under study.

Table 1
Level of irradiance (in W/m^2) on each module in Fig. 8.

	String 1	String 2
Position 1	1000	900
Position 2	600	500
Position 3	200	300

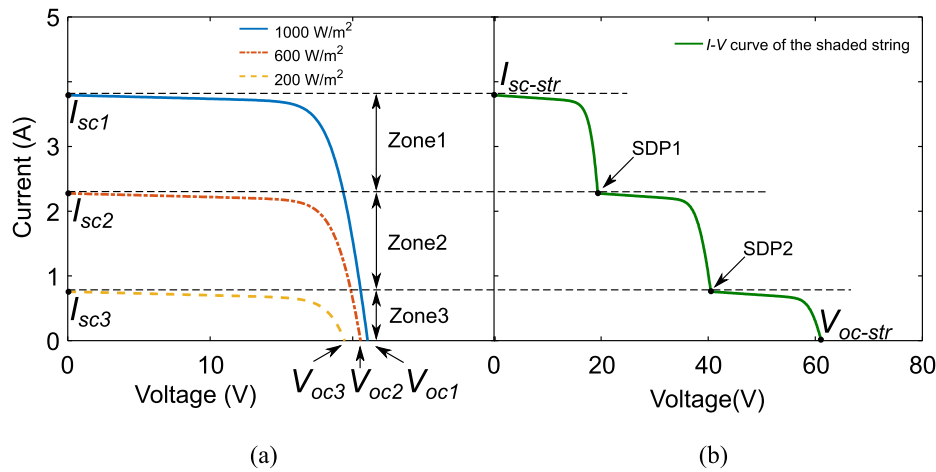


Fig. 9. (a) Plot of the I - V curves for each module. (b) A plot of the resulted I - V curve for the PV string shown in Fig. 10(a).

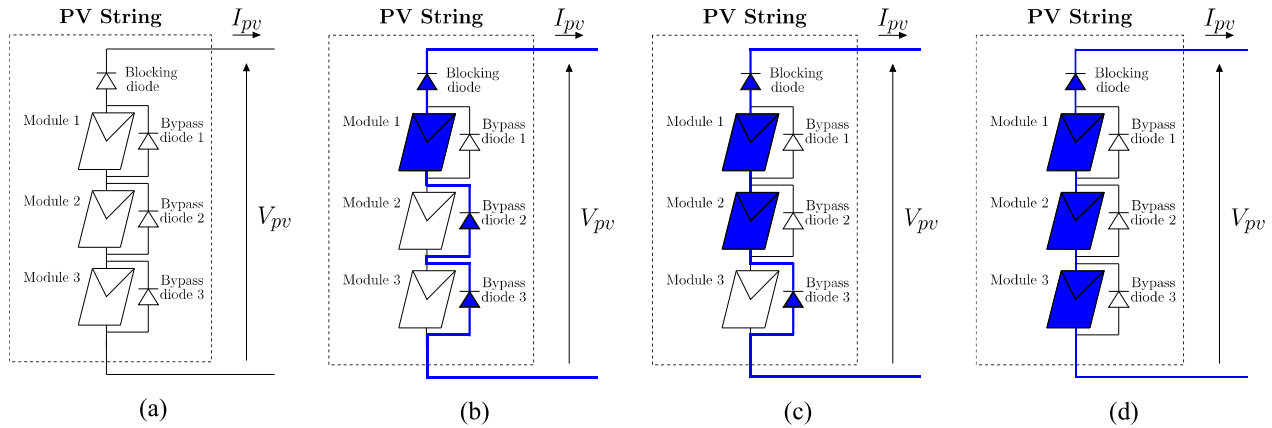


Fig. 10. (a) Typical connection of three series-connected PV string with bypass and blocking diodes. (a) Operation of the string in Zone 1: module 1 is generating current, and modules 2 and 3 are bypassed. (b) Operation in Zone 2: modules 1 and 2 are generating current, and module 3 is bypassed. (c) Operation in Zone 3: modules 1, 2, and 3 are generating current.

3. The proposed analytical modeling under partial shading

3.1. Principle of modeling of 2x3 PV array under partial shading

In this Section, the procedure used to obtain the I - V characteristics of shaded PV arrays is described. An illustrative example explains the behavior of a PV array composed of two parallel-connected strings, while each string composed of three series-connected modules is presented. The configuration of the PV array studied is described in Fig. 8.

Given a PV array consists of two parallel-connected strings, where each string is composed of three series-connected modules, as seen in Fig. 8. The irradiance level received by each module is given in Table 1.

To obtain the I - V characteristics of the shaded PV array shown in Fig. 7, the following steps are followed:

Step 1: the first step is to calculate the I - V characteristics of each module in the PV array, as explained in Section 2.

Step 2: the I - V curve for every string in the array is obtained. The I - V characteristics of the three modules of the first string ($str(1)$), under the same temperature but receiving different irradiance values given in Table 1, are shown in Fig. 9(a). Fig. 10(a) shows the string configuration with the insertion of bypass and blocking diodes. Fig. 9(b) shows the obtained I - V curve of the string. The section dividing point (SDP) is the point in the I - V curve at which the irradiance (thus the current) forms a step waveform. To understand how this curve is obtained, the current axis is divided into three zones. For each zone,

the operation is explained and the path of current inside the string is highlighted.

For a given string current ($I_{str(1)}$) in zone 1, i.e., $I_{sc1} < I_{str(1)} < I_{sc2}$, only module 1 generates current, and the remaining modules are bypassed, i.e., current flows through the bypass diodes connected in parallel with modules 2 and 3, as described in Fig. 10(b). The corresponding string voltage $V_{str(1)}(I_{str(1)})$ can be obtained using Eq. (12).

$$V_{str(1)}(I_{str(1)}) = V_{mod(1,1)}(I_{str(1)}) + V_{bypassD2}(I_{str(1)}) + V_{bypassD3}(I_{str(1)}) + V_{blockingD1}(I_{str(1)}) \quad (12)$$

Note that the calculation method of the voltage drop across the bypass ($V_{bypassD}$) and blocking diode ($V_{blockingD}$) will be presented in the next Section.

In zone 2, where $I_{sc2} < I_{str(1)} < I_{sc3}$, for a given string current $I_{str(1)}$, the current flows through modules 1 and 2 while module 3 is bypassed, as shown in Fig. 10(c). The corresponding string voltage $V_{str(1)}(I_{str(1)})$ can be written as in Eq. (13).

$$V_{str(1)}(I_{str(1)}) = V_{mod(1,1)}(I_{str(1)}) + V_{mod(2,1)}(I_{str(1)}) + V_{bypassD3}(I_{str(1)}) + V_{blockingD1}(I_{str(1)}) \quad (13)$$

When the operating point shifted to zone 3, i.e., $I_{sc3} < I_{str(1)} < 0$, all modules are conducting as seen in Fig. 10(d). The corresponding string voltage $V_{str(1)}(I_{str(1)})$ for a given string current ($I_{str(1)}$) in zone 3 can be written as in Eq. (14).

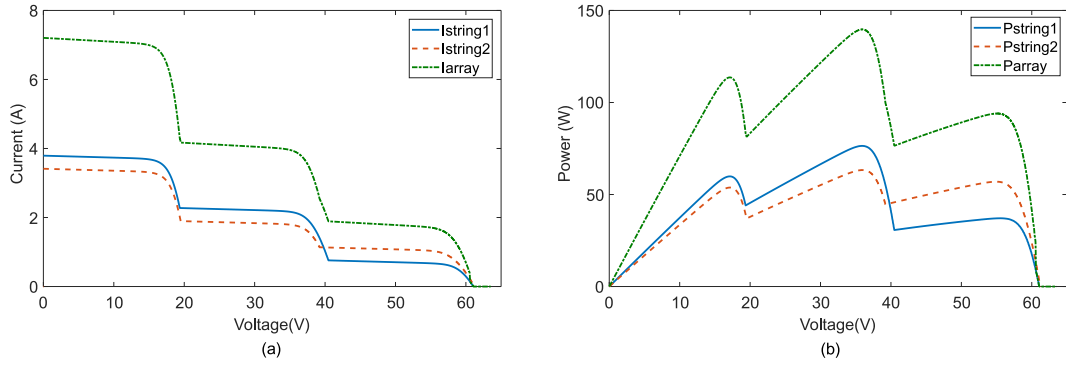


Fig. 11. Total (a) current and (b) power of the PV array of Fig. 8 obtained by summation of $I\text{-}V$ curves of strings 1 and 2.

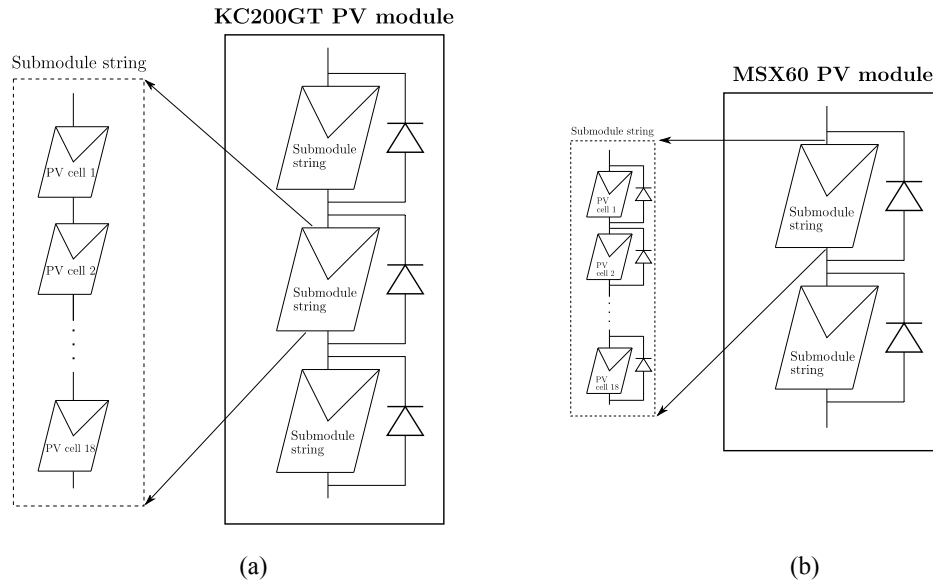


Fig. 12. (a). KC200GT PV panel consisting of three subpanel strings with three bypass diodes. Each subpanel string is composed of eighteen series-connected PV cells. (b). MSX60 PV panel consisting of two subpanel strings with 2 bypass diodes. Each subpanel string is composed of eighteen series-connected PV cells.

$$\begin{aligned} V_{str(1)}(I_{str(1)}) = & V_{mod(1,1)}(I_{str(1)}) + V_{mod(2,1)}(I_{str(1)}) + V_{mod(3,1)}(I_{str(1)}) \\ & + V_{blockingD1}(I_{str(1)}) \end{aligned} \quad (14)$$

In summary, the string voltage, for any given current, could be written as in Eq. (15).

The open-circuit voltage ($V_{oc\text{-array}}$) and the short circuit current ($I_{sc\text{-array}}$) of the array can be obtained using Eqs. (18) and (19), respectively.

$$I_{sc\text{-array}} = I_{sc\text{-str}(1)} + I_{sc\text{-str}(2)} \quad (18)$$

$$V_{oc\text{-array}} = \max(V_{oc\text{-str}(1)}, V_{oc\text{-str}(2)}) \quad (19)$$

$$V_{str(1)} = \begin{cases} V_{mod(1,1)}(I_{str(1)}) + 2 \times V_{bypassD}(I_{str(1)}) + V_{blockingD}(I_{str(1)}), & I_{str(1)} \in Zone1 : I_{SC1} \leq I_{str(1)} \prec I_{SC2} \\ V_{mod(1,1)}(I_{str(1)}) + V_{mod(2,1)}(I_{str(1)}) + V_{bypassD}(I_{str(1)}) + V_{blockingD}(I_{str(1)}), & I_{str(1)} \in Zone2 : I_{SC2} \leq I_{str(1)} \prec I_{SC3} \\ V_{mod(1,1)}(I_{str(1)}) + V_{mod(2,1)}(I_{str(1)}) + V_{mod(3,1)}(I_{str(1)}) + V_{blockingD}(I_{str(1)}), & I_{str(1)} \in Zone3 : I_{SC3} \leq I_{str(1)} \prec 0 \end{cases} \quad (15)$$

Step 3: Before deducing the electrical curves of the PV array, the short circuit current ($I_{sc\text{-str}(1)}$) of the string and the open-circuit voltage ($V_{oc\text{-str}(1)}$) need to be calculated using Eqs. (16) and (17), respectively.

$$I_{sc\text{-str}(1)} = \max(I_{sc1}, I_{sc2}, I_{sc3}) \quad (16)$$

$$V_{oc\text{-str}(1)} = V_{oc1} + V_{oc2} + V_{oc3} - V_{blockD1} \quad (17)$$

Step 4: The current of the PV array is calculated as follows: for any given array voltage point (V) between 0 and $V_{oc\text{-array}}$, the array current (I_{array}) is obtained by summation of all string currents using Eq. (20).

$$I_{array}(V) = I_{str1}(V) + I_{str2}(V) \quad (20)$$

For any given array voltage point (V) between 0 and $V_{oc\text{-array}}$, the corresponding array power (P_{array}) can be obtained using Eq. (21).

$$P_{array}(V) = I_{array}(V) \cdot V \quad (21)$$

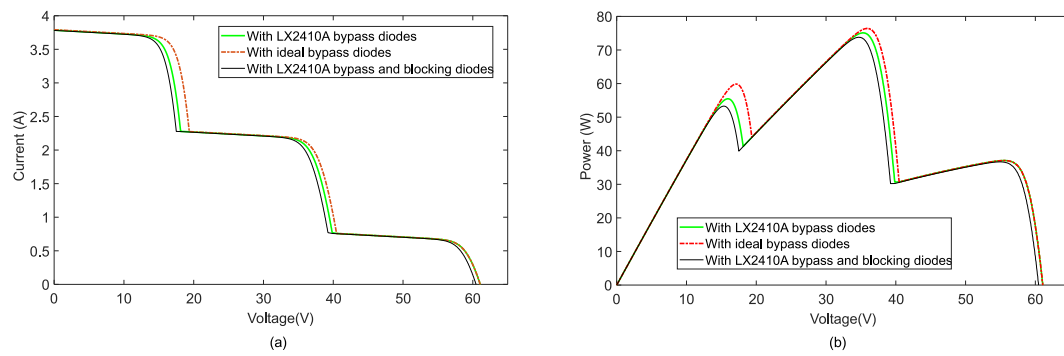


Fig. 13. Effect of the Bypass and the Blocking diodes on (a) I - V , and (b) P - V curves.

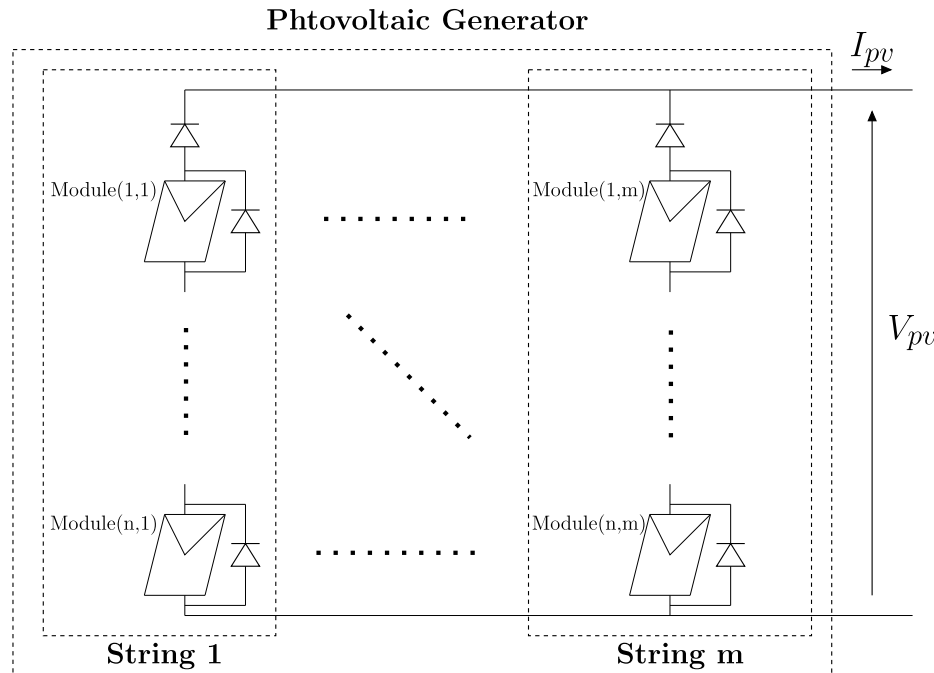


Fig. 14. The generalized PV array configuration: m is the number of strings while n is the number of series-connection of modules in each string.

Fig. 11 shows the I - V and P - V curves for each string and the resulted curves of the PV array of Fig. 7.

3.2. Effect of bypass and blocking diodes

The effect of bypass and blocking diodes on the electrical characteristics of shaded PV arrays is studied in this Section. In order to prevent hot-spot damage in a PV module, the number of solar cells bypassed by a diode is determined according to the breakdown voltage of the cells (V_{oc}) (Boztepe et al., 2014). Hence, the V_{oc} of the cells is obtained by dividing the rated open-circuit voltage of the PV module ($V_{oc,mod}$) by the number of bypass diodes across the module. For example, the Solarex MSX60 module (Solarex MSX60 and MSX64 Solar Arrays Datasheet, 1997) consists of 36 polycrystalline silicon solar cells electrically configured as two series strings of 18 cells each, which allows the installation of one bypass diode on each 18-cells string to avoid breakdown of PV cells during partial shading occurrence. The Kyocera KC200GT (Krismadinata et al., 2013) integrates 54 series-connected solar cells with three bypass diodes. Fig. 12 shows the internal configuration in KC200GT and MSX60 PV modules. Some manufacturers include six bypass diodes in large PV modules consist of 72 series-connected solar cells (Silvestre et al., 2009).

The bypass diode has its effect on the PV curve. When the diode is

conducting, Eq. (22) can be used to calculate the voltage across the diode (V_D).

$$V_D = V_{fwd} + R_{on}I_D \quad (22)$$

where V_{fwd} is the forward voltage of the diode, R_{on} is the equivalent on-resistance of the diode in conduction mode, and I_D is the current passes through the diode.

Fig. 13 shows the effect of the bypass and blocking diodes on the resulted I - V and P - V curves of the shaded string shown in Fig. 10. The dedicated LX2410A diode (Microsemi, 2015) is considered in this simulation test to compute the I - V and P - V curves. Three curves are plotted in this test, where the bypass and blocking diodes are considered ideal in the dashed red curve. Note that an ideal diode means that the diode is conducting with zero forward voltage and without any conduction losses, i.e., $V_{fwd} = 0$ and $R_{on} = 0$. In the second test resulted in the green solid line curve, the ideal bypass diodes are substituted by LX2410A bypass diodes while the blocking diode is considered ideal. In the last test resulting in the continuous black curve, all bypass and blocking diodes are real (Microsemi, 2015).

Although the voltage drop is tiny, the diodes have a remarkable effect on the resulted P - V curve. There is a power drop due to the effect of bypass and blocking diodes. In each peak, starting from the left-side

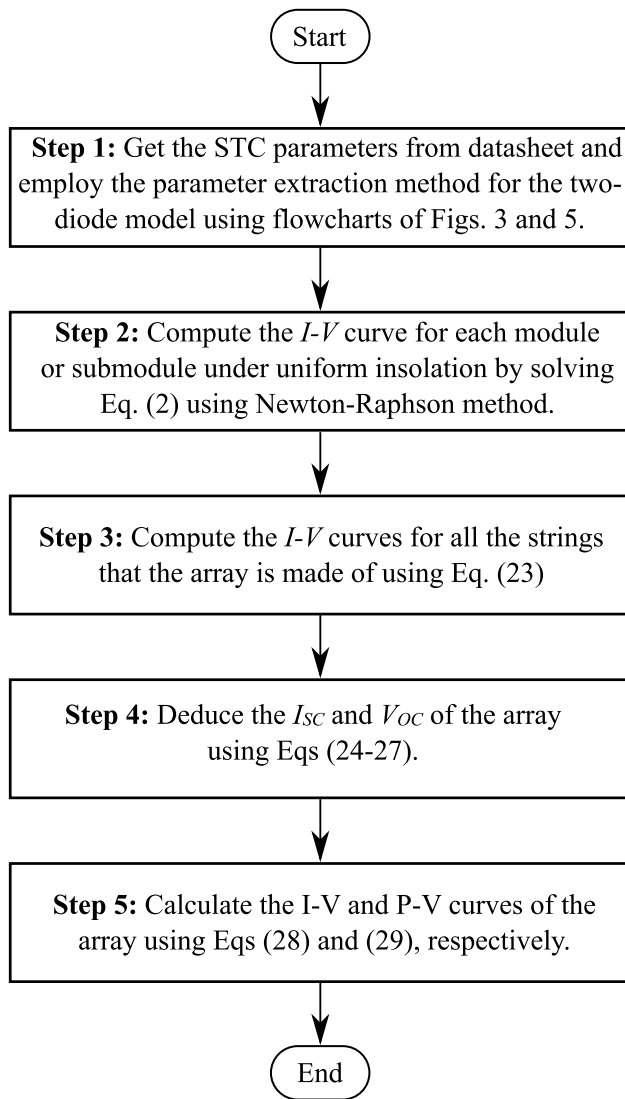


Fig. 15. The steps should be followed to compute the electrical characteristics of shaded PV arrays.

peak, the power drop is 11%, 3.5%, and 1.11%, respectively. A slight reduction of V_{oc-str} is observed due to the effect of the forward voltage of the blocking diode. $V_{oc-str} = 61.06$ V with ideal blocking diode, while it is 60.46 V with the real LX2410A blocking diode. The 0.6 V difference is due to the forward voltage of the blocking diode.

3.3. Generalized modeling approach for PV array under partial shading

The generalized approach to model the characteristics under partial shading conditions for any $n \times m$ series-parallel array configuration under any irradiance and temperature value is presented in this Section. A typical generalized PV array configuration is shown in Fig. 14.

A generalized formula that allows the calculation of $V_{str(j)}$ for any given string current $I_{str(j)}$ in any zone (z), while j varies from 1 to m , is given in Eq. (23).

$$V_{str(j)} = \sum_{i=1}^z V_{mod(i,j)}(I_{str(j)}) + \sum_{i=z+1}^n V_{bypassD}(I_{str(j)}) + V_{blockingD}(I_{str(j)}) \quad (23)$$

$\in Zone(z)$

Table 2

The shading profile for all shading patterns shown in Fig. 18.

Irradiance level (in W/m ²) on every module inside the string.	Number of series-connected modules in the PV string					
	3	6	9	12	15	1000
Position 1	1000	1000	1000	1000	1000	1000
Position 2	600	800	900	900	950	
Position 3	200	500	800	850	900	
Position 4	—	400	600	780	850	
Position 5	—	300	500	700	700	
Position 6	—	100	400	600	600	
Position 7	—	—	300	540	540	
Position 8	—	—	200	420	480	
Position 9	—	—	100	360	420	
Position 10	—	—	—	240	360	
Position 11	—	—	—	200	300	
Position 12	—	—	—	100	240	
Position 13	—	—	—	—	200	
Position 14	—	—	—	—	120	
Position 15	—	—	—	—	50	

The short circuit current ($I_{sc-str(j)}$) and the open-circuit voltage ($V_{oc-str(j)}$) of a string j , where $1 \leq j \leq m$, are calculated using Eqs. (24) and (25), respectively.

$$I_{sc-str(j)} = \max(I_{sc-str(1,j)}, I_{sc-str(2,j)}, \dots, I_{sc-str(n,j)}) \quad (24)$$

$$V_{oc-str(j)} = \sum_{i=1}^n V_{oc(i,j)} - V_{blockD} \quad (25)$$

The short circuit current ($I_{sc-array}$) and the open-circuit voltage ($V_{oc-array}$) of the array are calculated using Eqs. (26) and (27), respectively.

$$I_{sc-array} = \sum_{j=1}^m I_{sc-str(j)} \quad (26)$$

$$V_{oc-array} = \max(V_{oc-str(1)}, V_{oc-str(2)}, \dots, V_{oc-str(m)}) \quad (27)$$

For any given array voltage point (V) between 0 and $V_{oc-array}$, the array current (I_{array}) is obtained by summation of all string currents using Eq. (28).

$$I_{array}(V) = \sum_{j=1}^m I_{str(j)}(V) \quad (28)$$

The corresponding array power (P_{array}) for any given array voltage point (V) between 0 and $V_{oc-array}$ is given using Eq. (29).

$$P_{array}(V) = I_{array}(V) \cdot V \quad (29)$$

The flowchart of Fig. 15 is inserted to summarize the procedure of computing the electrical characteristics under a particular shading condition. The flowchart could also be used for coding purposes.

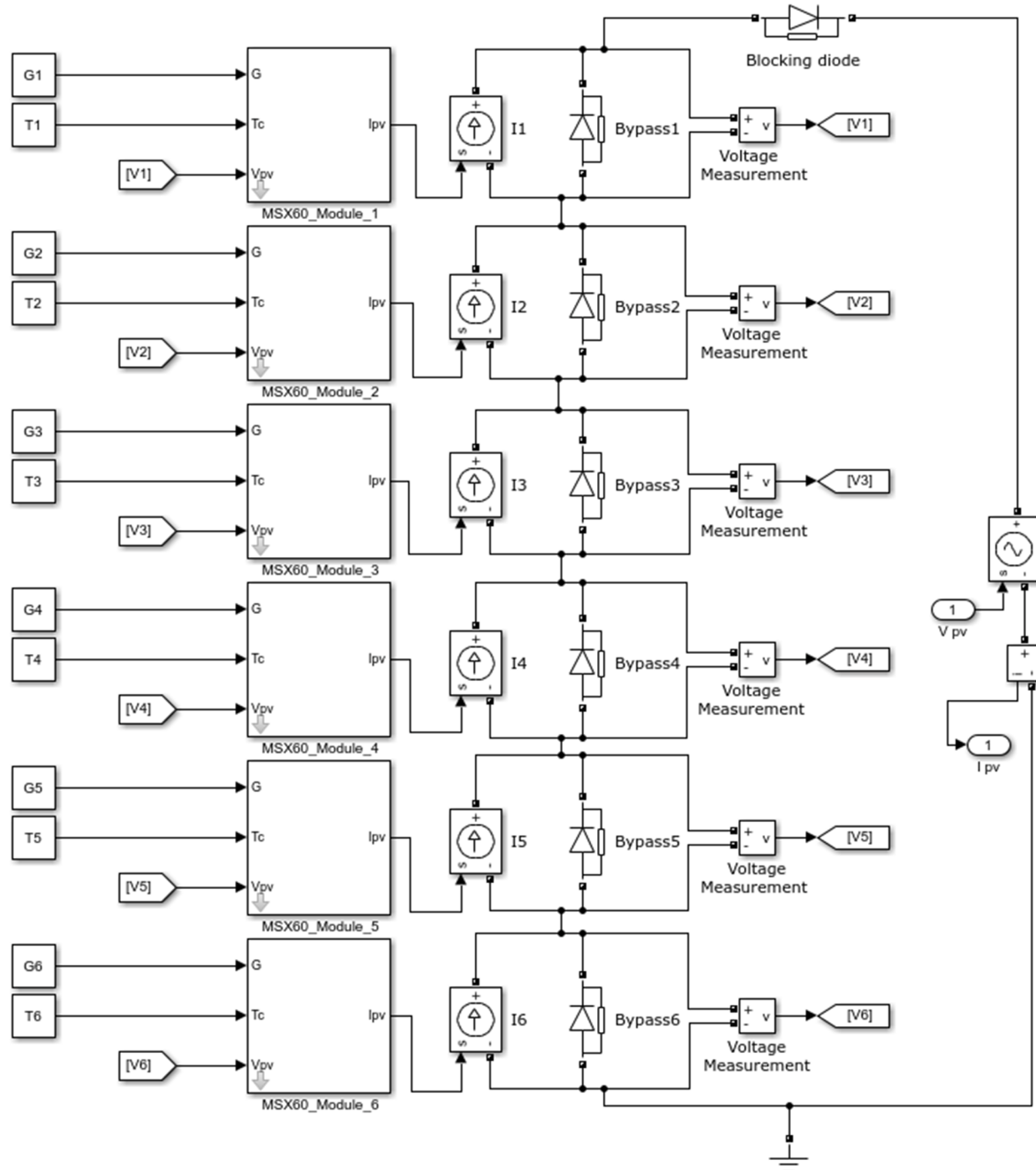


Fig. 16. Example of a component-based Simulink model used to plot the P-V curve of a string consisting of 6 series-connected modules under PSC.

4. Advantages of the proposed analytical approach over the component-based approach

To evaluate the execution time for both approaches: component-based and analytical-based, a series of simulation tests on strings of three, six, nine, twelve, and fifteen series-connected modules are considered. The PC workstation used for the test has an Intel(R) Core (TM) i5-4570 CPU @ 3.20 GHz with a RAM of 18.0 GB. The shading profiles for all PV strings considered for the test are listed in Table 2. For every test, both component-based and analytical-based approaches are evaluated under the same shading profile. The output characteristics of

the tested strings are computed using both approaches. For example, a component-based model of a PV string composed of six series-connected modules is shown in Fig. 16. While a Matlab-GUI that employs the proposed analytical-based approach for a PV string composed of twelve series-connected modules is depicted in Fig. 17. Through this GUI, the user can select the number of series-connected modules and change the irradiance level for any module in the string by changing the value of its corresponding slider.

For all string tests, The P-V curves are identically obtained from both component-based and analytical-based approaches, as shown in Fig. 18. However, there is a significant mismatch concerning the time needed for

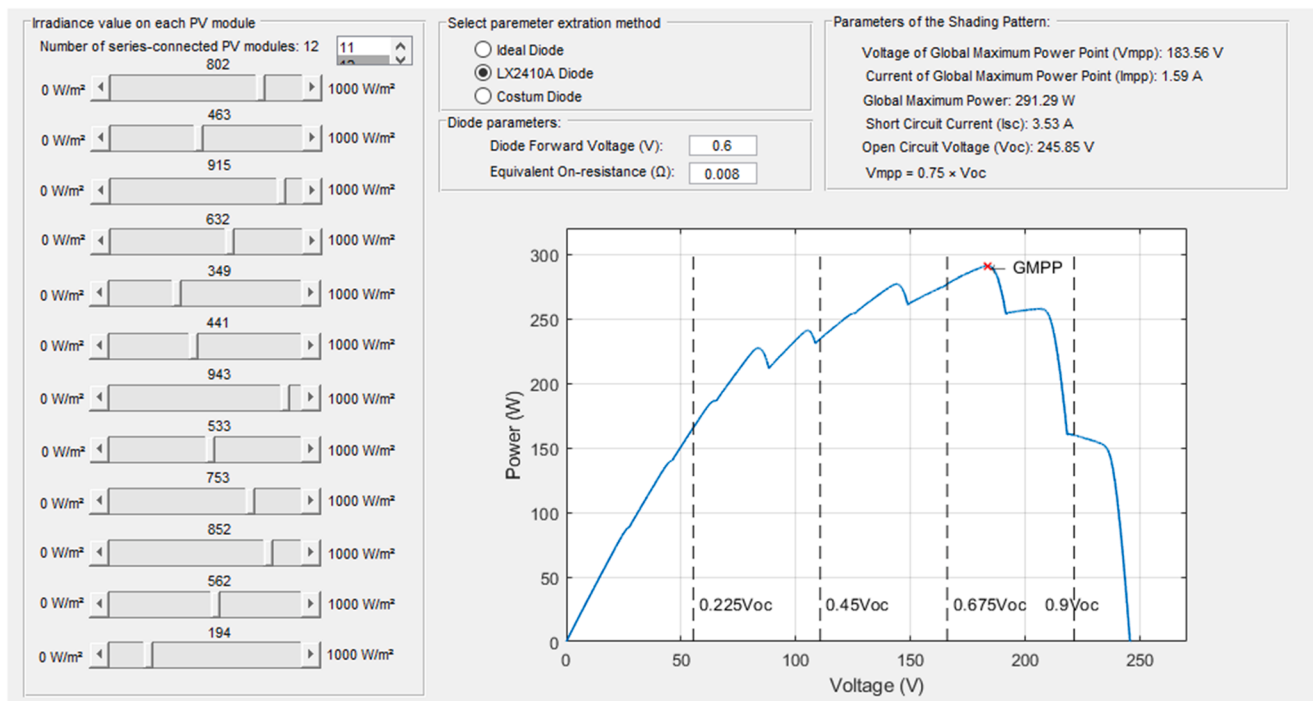


Fig. 17. Graphical-user interface developed to display the P-V characteristics of a PV string consisting of 12 series-connected modules. The proposed approach obtains the irradiance value of each module from the sliders and displays the calculated P-V curve.

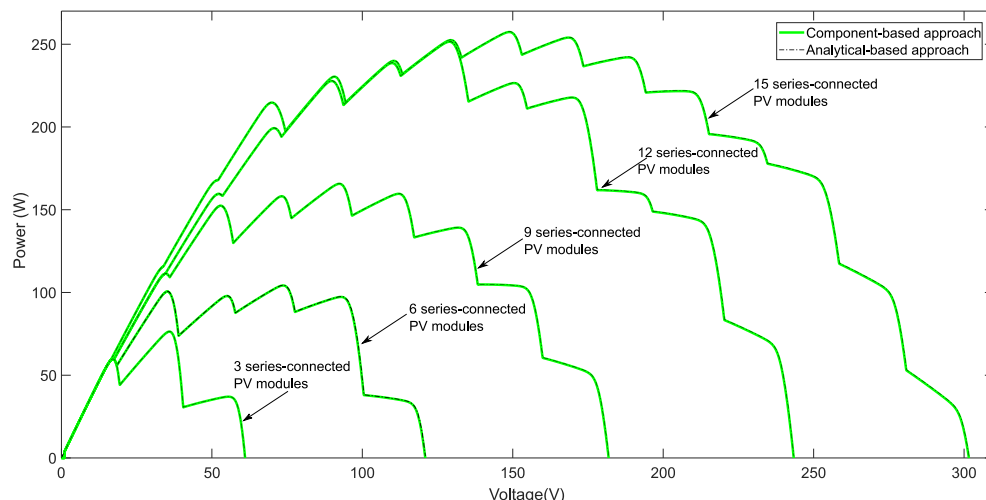


Fig. 18. A Plot of P-V curves using both methods under the same shading profile.

both programs to compute the outputs. As can be seen in Fig. 19, using the component-based approach, the simulation time increases roughly with the increase of the series-connected modules in the string. The proposed analytical approach is swift and can get the results on around one-tenth of the time needed by the Simulink model to complete the simulation run.

5. Conclusion

A generalized analytical method to obtain the I-V and P-V characteristics of a given PV array under any partial shading condition is presented in this paper. The two-diode model associated with the fast

parameter extraction method is used to draw the I-V curves of PV modules receiving the same quantity of irradiance inside the array. Then, these curves are manipulated to compute the curve of the whole PV array. The proposed generalized approach is fast and accurate and can be efficiently coded under any development environment. It enhances the prediction accuracy of the electrical characteristics of shaded PV arrays by incorporating the real effect of the blocking and bypass diodes in the proposed model. Furthermore, it can be generalized for any series-parallel array configuration under any irradiance distribution in the array. The proposed approach could be useful in many academic and professional domains.

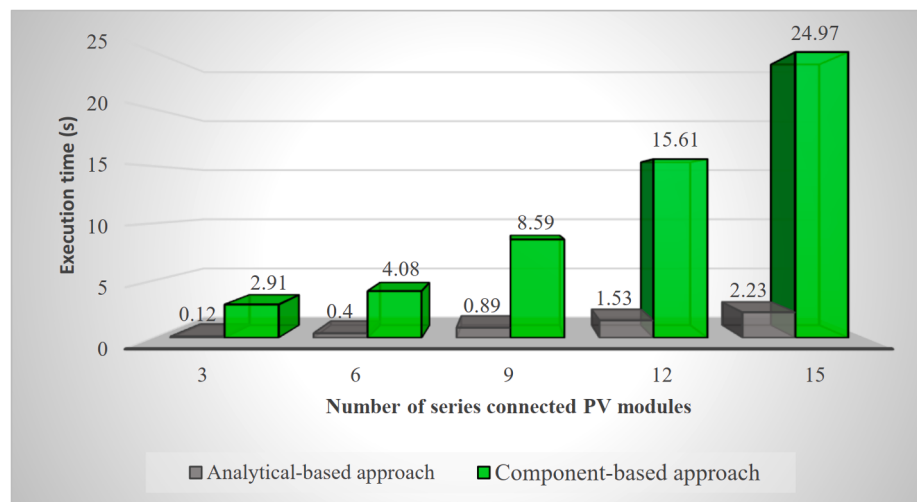


Fig. 19. Execution time needed for both approaches to computing the P-V curves shown in Fig. 18.

Declaration of Competing Interest

The authors declare that they have no known competing financial interests or personal relationships that could have appeared to influence the work reported in this paper.

Acknowledgement

The authors would like to thank University of Malaya, Malaysia, for providing financial support under the research grant Impact Oriented Interdisciplinary Research Grant (IIRG): IIRG011A-2019, Ministry of Higher Education, Malaysia under Large Research Grant Scheme (LRGS): LR008-2019 and Ministry of International Trade and Industry (MITI), Malaysia through MIDF under High Value Added and Complex Product Development and Market Program: GA016-2019.

Appendix A. Supplementary material

Supplementary data to this article can be found online at <https://doi.org/10.1016/j.solener.2020.07.077>.

References

- Arjun, M., Ramana, V.V., Viswadev, R., Venkatesaperumal, B., 2019. An iterative analytical solution for calculating maximum power point in photovoltaic systems under partial shading conditions. *IEEE Trans. Circuits Syst. II Express Briefs* 66 (6), 973–977. <https://doi.org/10.1109/TCSII.2018.2867088>.
- Boztepe, M., Guinjoan, F., Velasco-Quesada, G., Silvestre, S., Chouder, A., Karatepe, E., 2014. Global MPPT scheme for photovoltaic string inverters based on restricted voltage window search algorithm. *IEEE Trans. Ind. Electron.* 61 (7), 3302–3312. <https://doi.org/10.1109/TIE.2013.2281163>.
- Chih-Tang, S., Noyce, R.N., Shockley, W., 1957. Carrier generation and recombination in P-N junctions and P-N junction characteristics. *Proc. IRE* 45 (9), 1228–1243. <https://doi.org/10.1109/JRPROC.1957.278528>.
- Chin, V.J., Salam, Z., 2018. Modifications to Accelerate the iterative algorithm for the two-diode model of PV module. In: 2018 IEEE PES Asia-Pacific Power and Energy Engineering Conference (APPEEC). IEEE, pp. 200–205.
- Chin, V.J., Salam, Z., Ishaque, K., 2015a. An improved method to estimate the parameters of the single diode model of photovoltaic module using differential evolution. In: Electric Power and Energy Conversion Systems (EPECS), 2015 4th International Conference on, 24–26 Nov. 2015, pp. 1–6, doi: 10.1109/epecs.2015.7368514. [Online]. Available: [http://ieeexplore.ieee.org/ielx7/7364554/7368488/pdf?tp=&arnumber=7368488](http://ieeexplore.ieee.org/ielx7/7364554/7368488/pdf?tp=&arnumber=7368514&isnumber=7368488).
- Chin, V.J., Salam, Z., Ishaque, K., 2015b. An accurate two diode model computation for CIS thin film PV module using the hybrid approach. In: Electric Power and Energy Conversion Systems (EPECS), 2015 4th International Conference on, 24–26 Nov. 2015, pp. 1–6, doi: 10.1109/epecs.2015.7368493. [Online]. Available: <http://ieeexplore.ieee.org/ielx7/7364554/7368488/pdf?tp=&arnumber=7368493&isnumber=7368488>.
- Chin, V.J., Salam, Z., Ishaque, K., 2015c. Cell modelling and model parameters estimation techniques for photovoltaic simulator application: A review. *Appl. Energy* 154, 500–519. <https://doi.org/10.1016/j.apenergy.2015.05.035>.
- Chin, V.J., Salam, Z., Ishaque, K., 2016. An accurate modelling of the two-diode model of PV module using a hybrid solution based on differential evolution. *Energy Convers. Manage.* 124 <https://doi.org/10.1016/j.enconman.2016.06.076>.
- Chin, V.J., Salam, Z., Ishaque, K., 2017a. An accurate and fast computational algorithm for the two-diode model of PV module based on a hybrid method. *IEEE Trans. Ind. Electron.* 64 (8), 6212–6222. <https://doi.org/10.1109/TIE.2017.2682023>.
- Chin, V.J., Salam, Z., Ishaque, K., 2017b. An accurate and fast computational algorithm for the two-diode Model of PV module based on hybrid method. *IEEE Trans. Ind. Electron.* 64 (8), 6212–6222. <https://doi.org/10.1109/TIE.2017.2682023>.
- Chin, V.J., Salam, Z., 2019. Coyote optimization algorithm for the parameter extraction of photovoltaic cells. *Sol. Energy* 194, 656–670. <https://doi.org/10.1016/j.solener.2019.10.093>.
- Dadié, A., Djongyang, N., Tchinda, R., 2018. An analytical-numerical approach in the calculation of photovoltaic module parameters operating under partial shaded conditions. *Afr. J. Sci. Technol. Innovat. Develop.* 10 (6), 701–707. <https://doi.org/10.1080/20421338.2018.1491677>.
- Diqing, Z., Wu, C., Li, Z., 2012. Modeling and simulation of partial shaded PV modules. In: Xiao, T., Zhang, L., Ma, S. (Eds.), *System Simulation and Scientific Computing*. Springer, Berlin Heidelberg, pp. 124–134.
- Ishaque, K., Salam, Z., Syafaruddin, 2011a. A comprehensive MATLAB Simulink PV system simulator with partial shading capability based on two-diode model. *Sol. Energy* 85 (9), 2217–2227. <https://doi.org/10.1016/j.solener.2011.06.008>.
- Ishaque, K., Salam, Z., Taheri, H., 2011b. Simple, fast and accurate two-diode model for photovoltaic modules. *Sol. Energy Mater. Sol. Cells* 95 (2), 586–594. <https://doi.org/10.1016/j.solmat.2010.09.023>.
- Jing Jun, S., Kay-Soon, L., 2012. Photovoltaic model identification using particle swarm optimization with inverse barrier constraint. *IEEE Trans. Power Electron.* 27 (9), 3975–3983. <https://doi.org/10.1109/TPEL.2012.2188818>.
- Krismadinata, Rahim, N.A., Ping, H.W., Selvaraj, J., 2013. Photovoltaic Module Modeling Using Simulink/Matlab. *Procedia Environ. Sci.* 17 (0), 537–546. <https://doi.org/10.1016/j.proenv.2013.02.069>.
- Microsemi, 2015. LX2410A 10A IDEALTM Bypass Device.
- Patel, H., Agarwal, V., 2008. MATLAB-based modeling to study the effects of partial shading on PV array characteristics. *IEEE Trans. Energy Convers.* 23 (1), 302–310. <https://doi.org/10.1109/TEC.2007.914308>.
- Prasanth Ram, J., Pillai, D.S., Rajasekar, N., Kumar Chinnaiyan, V., 2020. Flower pollination based solar PV parameter extraction for double diode model. In: Kalam, A., Niazi, K.R., Soni, A., Siddiqui, S.A., Mundra, A. (Eds.), *Intelligent Computing Techniques for Smart Energy Systems*. Singapore: Springer, Singapore, pp. 303–312.
- Quaschning, V., Hanitsch, R., 1996. Numerical simulation of current-voltage characteristics of photovoltaic systems with shaded solar cells. *Sol. Energy* 56 (6), 513–520. [https://doi.org/10.1016/0038-092X\(96\)00006-0](https://doi.org/10.1016/0038-092X(96)00006-0).
- Seyedmahmoudian, M., Mekhilef, S., Rahmani, R., Yusof, R., Renani, T.E., 2013. Analytical modeling of partially shaded photovoltaic systems. *Energies* 6 (1). <https://doi.org/10.3390/en6010128>.
- Shukla, A.K., Sudhakar, K., Baredar, P., 2017. Recent advancement in BIPV product technologies: A review. *Energy Build.* 140, 188–195. <https://doi.org/10.1016/j.enbuild.2017.02.015>.
- Silvestre, S., Boronat, A., Chouder, A., 2009. Study of bypass diodes configuration on PV modules. *Appl. Energy* 86 (9), 1632–1640. <https://doi.org/10.1016/j.apenergy.2009.01.020>.
- Solarex MSX60 and MSX64 Solar Arrays Datasheet, 1997. <http://www.solarelectricsupply.com/solarex-msx-60-w-junction-box-548>.

- Villalva, M.G., Gazoli, J.R., Filho, E.R., 2009. Comprehensive approach to modeling and simulation of photovoltaic arrays. *IEEE Trans. Power Electron.* 24 (5), 1198–1208. <https://doi.org/10.1109/TPEL.2009.2013862>.
- Walker, G., 2001. Evaluating MPPT converter topologies using a MATLAB PV model. *J. Electr. Electron. Eng., Australia* 21 (1), 49.
- Wang, Y., Hsu, P., 2010. Analytical modelling of partial shading and different orientation of photovoltaic modules. *IET Renew. Power Gener.* 4 (3), 272–282. <https://doi.org/10.1049/iet-rpg.2009.0157>.
- Xenophontos, A., Bazzi, A.M., 2018. Model-based maximum power curves of solar photovoltaic panels under partial shading conditions. *IEEE J. Photovoltaics* 8 (1), 233–238. <https://doi.org/10.1109/JPHOTOV.2017.2764488>.